Z. Phys. B – Condensed Matter 82, 129–134 (1991)

Condensed
Zeitschrift für Physik B Matter

Critical behavior of the site percolation model on the square lattice in a $L \times M$ geometry

Monte Carlo and finite-size scaling study

R.A. Monetti and E.V. Albano *

Instituto de Investigaciones Fisicoquímicas Teóricas y Aplicadas (INIFTA), Facultad de Ciencias Exactas, Universidad Nacional de La Plata, Suc. 4, C.C. 16, (1900) La Plata, Argentina

Received June 27, 1990

Relevant aspects of the critical behavior of the site percolation model in a $L \times M$ geometry ($L \ll M$) are studied. It is shown that this geometry favors the growth of percolating clusters in the L-direction with respect to those growing in the M-direction, causing pronounced finite-size effects on the percolation probabilities. Scaling functions have an additional parameter, namely M, which introduces a dependence of these functions on the aspect ratio L/M. At criticality, the probability of a site belonging to the percolation clusters ($P_{L,M}$) behaves like $P_{L,M} \propto L^{-\beta/\nu} \phi(L/M)$ with $\beta = 5/36$ and $\nu = 4/3$, where ϕ is a suitable scaling function. Using scaling arguments it is conjectured and then tested by means of Monte Carlo simulations, the following asymptotic behavior $\phi(L/M) \propto (L/M)^{\delta}$, ($L \to \infty$, $M \to \infty$, $\delta = 1$), for the leading term. Systematic deviations of the Monte Carlo data from the conjectured behavior are due to second order corrections to the leading term which can also be understood on the basis of scaling ideas. Finite-size dependent "critical probabilities" are also functions of L/M as it follows from scaling arguments which are corroborated by the simulations.

I. Introduction

The percolation theory and percolation models are topics of permanent research due to their interesting applications in many fields of experimental and theoretical physics and physical-chemistry (see for example the reviews [1–6] and references therein). Percolation problems are studied by means of a number methods and techniques such as for example the percolative renormalization group [3], finite-size scaling [3, 5–7], Monte-Carlo simulations [3, 7–9], etc. Particularly, finite-size effects in the standard percolation model (henceforth SPM) on the square lattice in two dimensions (2D) have been extensively studied using a $L \times L$ geometry (L = lattice size) and assuming periodic boundary conditions [1–9] or occasionally free boundary conditions [7]. The aim of the present work is to study some relevant aspects of the critical behavior of the SPM on the square lattice assuming the $L \times M$ ($L \ll M$) geometry. The lack of studies of the SPM on a $L \times M$ geometry (within our best knowledge) is in contrast with extensive investigations of the Ising model on such geometry (see for example [10–12] and references therein).

The investigation is based upon Monte-Carlo simulations and finite-size scaling arguments. It is expected that the present study will be useful for the understanding of finite-size effects on the behavior of adsorbed monolayers on stepped surfaces assuming random adsorption on terraces L-lattice spacings wide. In fact, since substrata atoms at step sites account for the major contribution to structural defects in single crystal surfaces, the influence of steps on adsorption phenomena has been experimentally [13–17] and theoretically [10–12, 18, 19] investigated with growing attention (for a review see also reference [20]). The present study would also be useful to qualitatively understand some properties of media constituted by consecutive layers; where for $L \ll M$, L becomes the only relevant dimension; such as for example diffusion and conductivity [6] in layered compounds, the flow of immiscible fluids [6] in layered porous media, etc.

The manuscript is organized as follows: in Sect. II a brief description of the SPM and the simulation method in presented. Finite-size scaling arguments are given in Sect. III, the results are presented and discussed in Sect. IV and the conclusions are stated in Sect. V.

II. Brief description of the SPM and the Monte Carlo method

Details on the SPM in 2D have been already published [1–9], so let us recall that the square lattice with a $L \times M$

* Financially supported by the Consejo Nacional de Investigaciones Científicas y Técnicas (CONICET) de la República Argentina

geometry is filled at random with probability p. A cluster is a group of particles connected by nearest-neighbor (n−n) bonds. It has been established that, in the thermodynamic limit, there is a critical probability ($p_c \cong 0.59275 \pm 0.00003$ [3]) such us for $p < p_c$ clusters are confined to finite regions while just at $p = p_c$ a percolation cluster (i.e. the so called incipient percolation cluster (IPC)) appears for the first time.

The Monte-Carlo simulations are performed assuming free boundary conditions in both the M and L-directions. Under this assumption, clusters are identified using standard algorithms [3]. Results are typically averaged over 10^3–10^5 different configurations, depending on the lattice size, in order to achieve reasonable statistics.

Let us note that the study is restricted to single (independent) $L \times M$ samples, which is consistent with the assumption of random occupancy of lattice sites. So, this restriction implies absence of interactions between, on one hand absorbed species at neighboring terraces and on the other hand, diffusing particles on different layers of the layered sample.

III. Theoretical background on finite-size scaling

III.a. The largest cluster close to p_c

In order to analyze some relevant properties of the IPC let us define the probability $P_\infty(p)$ of a site belonging to the infinite cluster as a function of p. In the thermodynamic limit it holds [3–7]

$$P_\infty(p) \propto (p - p_c)^\beta \qquad L = \infty, p > p_c, p \to p_c, \tag{1}$$

with $\beta = 5/36$ in 2D. Working with finite ($L \times L$) lattices one determines the probability of a site belonging to the largest cluster $P_L(p)$ and it is necessary to use finite-size scaling arguments to analyze the data. So, one has [3, 7]

$$P_L(p) \propto \phi(L, \xi) \propto L^{-\beta/\nu} \hat{\phi}((p - p_c) L^{1/\nu}) \tag{2}$$

where ϕ and $\hat{\phi}$ are suitable scaling functions and $\nu = 4/3$ is the correlation length exponent; viz. the correlation length ξ in the infinite system behaves as

$$\xi \propto (p - p_c)^{-\nu}. \tag{3}$$

In the $L \times M$ geometry one has an additional scaling variable, so

$$P_{L,M}(p) \propto \phi_1(L, M, \xi) \propto L^{-\beta/\nu} \hat{\phi}_1\left(\frac{L}{M}, (p - p_c) L^{1/\nu}\right) \tag{4}$$

where ϕ_1 and $\hat{\phi}_1$ are also suitable scaling functions. Note that working with a constant aspect ratio L/M, Eq. (1) is recovered from (4) assuming the following asymptotic behavior

$$\hat{\phi}_1(L/M, (p - p_c) L^{1/\nu}) \propto \{(p - p_c) L^{1/\nu}\}^\beta,$$
$$L/M = \text{cte}, \quad M, L \to \infty. \tag{5}$$

The existence of two scaling variables in (4) allows us to study the dependence of $P_{L,M}(p)$ on the aspect ratio by keeping constant $\varepsilon \equiv (p - p_c) L^{1/\nu}$. In this case and right at criticality the second variable vanishes and we conjectured the following behavior of the scaling function

$$\hat{\phi}_1(L/M, 0) \propto (L/M)^\delta, \quad L, M \to \infty, \quad p = p_c. \tag{6}$$

In order to estimate the exponent δ one has to use the fact that the IPC has a fractal structure and the average mass $M(p = p_c)$ of this cluster depends on L as

$$M(p = p_c) \propto L^{D_F}, \quad L \to \infty, \tag{7a}$$
$$D_F = d - \beta/\nu = 91/48, \quad (2\text{D}). \tag{7b}$$

Now using the approximation $M(p = p_c) \propto P_{L,M}(p_c)$. LM and replacing $P_{L,M}(p_c)$ by (4) and (6), one has

$$M(p = p_c) \propto L^{-\beta/\nu} \left(\frac{L}{M}\right)^\delta LM$$
$$= L^{1+\delta-\beta/\nu} M^{1-\delta} \propto L^{D_F} \qquad L, M \to \infty. \tag{8}$$

Then, using (7b) it follows that $\delta = d - 1$ in d-dimensions, so $\delta = 1$ in $2D$.

III.b. The percolation probability

The percolation probability P.P.(p), is defined as the probability to find a percolation cluster for a given value of p. In the thermodynamic limit one has that P.P.(p) = 0 for $p < p_c$ and P.P.(p) = 1 for $p \geqq p_c$. Nevertheless, for finite systems, one expects in principle, a no-vanishing value of P.P.(p) for all p (P.P.(p) ≠ 0 for $0 < p \leqq 1$, see Fig. 1 Sect. IV) and consequently it is only possible to determine lattice-size-dependent values of the "critical probability" (say $p_c(L)$ for $L \times L$ systems) [3, 8]. Using finite-size scaling arguments it follows that [3, 8]

$$p_c = p_c(L) + AL^{-1/\nu} \tag{9}$$

where A is a constant. Working with a $L \times M$ geometry one can determine the percolation probabilities in the L and M-directions and their respective finite-size-dependent critical probabilities $p_{cL}(L, M)$ and $p_{cM}(L, M)$. So, like in the previous analysis of the larger cluster properties, there is an additional scaling variable (namely M) and (9) becomes

$$p_{cL}(L, M) = p_c + C_1(L/M) L^{-1/\nu}, \tag{10a}$$
$$p_{cM}(L, M) = p_c + C_2(L/M) M^{-1/\nu}, \tag{10b}$$

where C_1 and C_2 are constants for fixed values of the aspect ratio.

In order to symmetrize (10a) we conjectured that

$$C_1(L/M) = C_{l0} + C_l(L/M)^\alpha, \quad L, M \to \infty. \tag{11}$$

Replacing Eq. (11) in (10a) it follows

$$p_{cL}(L, M) = p_c + C_{l0} L^{-1/\nu} + C_l L^{\alpha - 1/\nu} M^{-\alpha}. \tag{12}$$

Now, Eq. (12) becomes symmetric under the interchange of the lattice dimensions by setting $\alpha = 1/\nu$. Note

that (9) can be recovered from (12) for $M=L$. Similar arguments can also be used in order to symmetrize (10b), i.e.

$$p_{cM}(L, M)=p_c+C_{m0}\,M^{-1/\nu}+C_m L^{-1/\nu}. \quad (13)$$

Comparing Eq. (12) and (13) it follows that $C_m=C_l$ and $C_{l0}=C_{m0}$ in order to be consistent with the symmetry of the problem.

IV. Results and discussion

IV.a. The percolation probability

Figure 1 shows the percolation probabilities P.P.$_L(p)$ and P.P.$_M(p)$ in the L and M-directions of the lattice, respectively, as a function of p for a system of size $L=6$, $M=48$. A comparison between these results and the behavior corresponding to the thermodynamic limit, i.e. a step right at p_c, shows up the existence dramatic finite-size effects such as rounding and shifting of the transition. The shift of both P.P.$_L(p)$ and P.P.$_M(p)$ to the left and the right side with respect to p_c, respectively, can be qualitatively understood after inspection of snapshot figures of the system taken at different values of p (Fig. 2). In fact, for $p=0.40$ one has only no-percolating clusters in Fig. 2a. At $p=0.50$, Fig. 2b shows that a percolating cluster in the L-direction has been already growth. At $p=p_c$ and due to the constraint $L\ll M$, one observes the growth of numerous percolation clusters along the L-direction (four clusters in Fig. 2c). On the other hand, the development of a single percolation cluster along the M-direction mostly occurs for $p>p_c$ (Fig. 2e for $p=0.70$), but even for this high value of p one can find configurations with clusters percolating in the L-direction only (Fig. 2d). It is interesting to compare these results with Monte-Carlo simulations of the ferromagnetic Ising model on the $L\times M$ geometry is absence of both surface and bulk magnetic fields [10] (Fig. 3). In fact, while at low temperature ($T\leqq 0.85\,T_c$, where T_c is the critical temperature) the system exhibits spin domains with a very large typical length in the M-direction, this typical length decreases rapidly as one approaches T_c and becomes there of the order of L. So, on one hand for the Ising model close to T_c one has patterns of spin-up domains (high-coverage islands) followed by spin-down domains (low-coverage islands) while, on the other hand for the SPM close to p_c the snapshots show a sequence of percolating clusters alternated by regions having smaller (no-percolating) clusters.

In order to analyze more quantitatively the observed finite-size effects one has to find out a method suitable to measure both $p_{cL}(L, M)$ and $p_{cM}(L, M)$, that is the finite-size-dependent "critical probabilities". According to previous works these thresholds are defined by demanding [8, 9], P.P.$_L(p_{cL})\equiv 0.9$ and P.P.$_M(p_{cM})\equiv 0.9$, respectively. Figure 4 shows plots of p_{cL} and p_{cM} vs $L^{-1/\nu}$ and $M^{-1/\nu}$, respectively, for different values of the aspect ratio L/M. Straight lines are only obtained for each set of points with the same aspect ratio, in agreement with

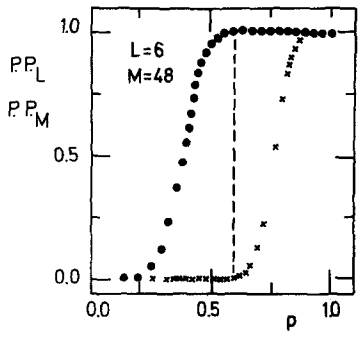

Fig. 1. Plots of the percolation probabilities in the L and M-directions of the lattice (●) P.P.$_L$ and (×) P.P.$_M$, respectively, versus the site occupation probability p. Results averaged over 10^5 different configurations for the lattice size $L=6$, $M=48$. The dashed line shows the stepped transition characteristic of the SPM in the thermodynamic limit right at p_c

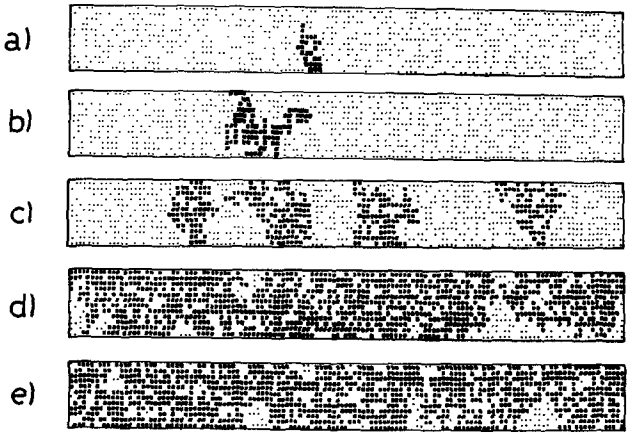

Fig. 2a–e. Typical snapshot configurations for rectangular samples of size $L=12$, $M=132$ at different values of the occupation probability p. Sites taken by both, the largest and percolating clusters, are shown in black squares, other occupied sites are shown in black points and empty sites are left white. **a** $p=0.40$, **b** $p=0.50$, **c** $p=p_c$, **d** $p=0.70$ showing two percolating clusters in the L-direction and **e** $p=0.70$ with a single percolating clusters in the M-direction. More details in the text

Fig. 3a–c. Snapshot pictures of a $L=24$, $M=288$ ferromagnetic Ising lattice in absence of both surface and bulk magnetic fields and temperatures $T=0.95\,T_c$ (**a**), $T=T_c$ (**b**) and $T=1.05\,T_c$ (**c**); where T_c is the critical temperature. Lattices sites taken by an up spin are indicated by a black square, others are left white. The configurations shown resulted after 18.000 Monte-Carlo steps per spin. (Taken from reference [10])

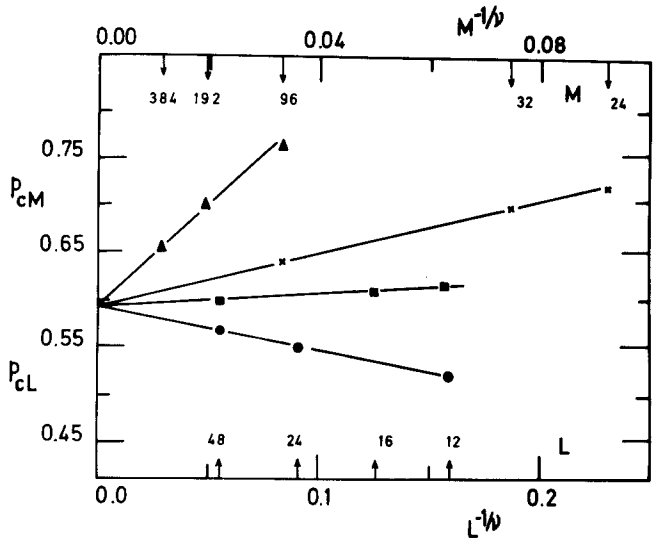

Fig. 4. Plots of the finite-size-dependent "critical probabilities" $p_{cL}(p_{cM})$ in the $L(M)$-direction versus $L^{-1/\nu}(M^{-1/\nu})$ for systems with different aspects ratio (■) $L/M=1/2$, (●) $L/M=1/8$; ((×) $L/M=1/2$, (▲) $L/M=1/8$), respectively. The corresponding width and length of the lattice is shown by arrows in the lower and upper part of the figure, respectively

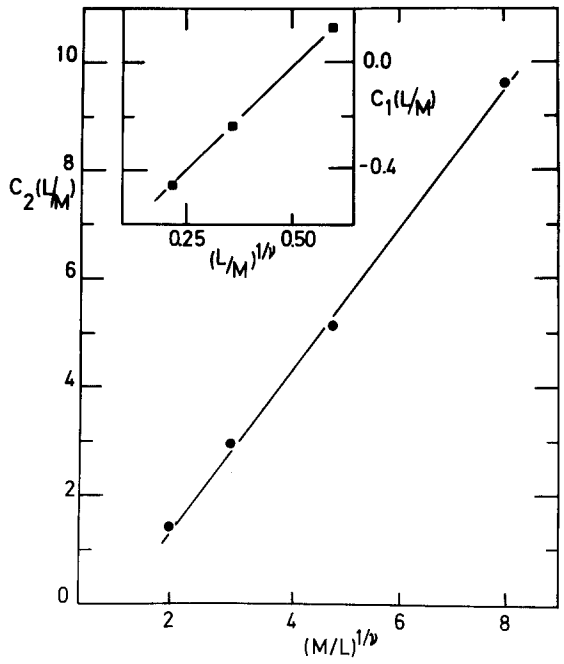

Fig. 5. Plot of $C_2(L/M)$ versus $(M/L)^{1/\nu}$. Data obtained from the slopes of straight lines like those shown in Fig. 4. The aspect ratio of the lattices are, from the left to the right hand: $L/M=1/2$, 1/4, 1/8 and 1/16. The inset shows a plots of $C_1(L/M)$ versus $(L/M)^{1/\nu}$ for the following aspect ratio of the lattices, from left to right: $L/M=1/8$, 1/4 and 1/2

Table 1. Values of the critical probability obtained extrapolating p_{cL} and p_{cM} to $L\to\infty$ and $M\to\infty$, respectively, for lattices of different aspect ratio L/M. The last two lines shown the values of p_c obtained from the plots of $p_{cL}(L, M)$ vs $X(L, M)$ and $p_{cM}(L, M)$, respectively (see Fig. 6a–b)

L/M	$p_c(L\to\infty)$	$p_c(M\to\infty)$
1/2	0.593	0.594
1/4	0.594	0.594
1/8	0.594	0.597
1/16	0.591	0.599
$X(L, M)=0$	0.5927	–
$Y(L, M)=0$	–	0.5922

(10a, b). Furthermore, the extrapolations $p_{cL}(L\to\infty)$ and $p_{cM}(M\to\infty)$ give values of p_c which are in good agreement with the best available value of the critical probability, i.e. $p_c=0.59275\pm0.00003$ [3] as it follows from Table 1. In order to test our conjecture (Eq. (11) with $\alpha=1/\nu$), the slopes of the straight lines obtained from Fig. 4 and similar plots for different values of the aspects ratio (not shown here) are plotted against $(L/M)^{1/\nu}$ in Fig. 5. This figure suggests that the conjecture holds for both $C_1(L/M)$ and $C_2(L/M)$ and from the obtained straight lines one gets $C_{l0}\simeq-0.77$, $C_l\simeq1.53$, $C_{m0}\simeq-0.81$ and $C_m\simeq1.30$. Note that $C_{l0}\simeq C_{m0}$ and $C_l\simeq C_m$ within error bars of 5% and 15%, respectively, which is reasonable taking not only the errors of the Monte Carlo simulations but also the method used to calculate the C-values into account. Now, knowing these constants one can also test the validity of (12) and (13). In fact, defining

$$X(L, M)\equiv C_{l0}\,L^{-1/\nu}+C_l\,M^{-1/\nu} \tag{14a}$$

$$Y(L, M)\equiv C_{m0}\,M^{-1/\nu}+C_m\,L^{-1/\nu} \tag{14b}$$

one has that plots of $p_{cL}(L, M)$ and $p_{cM}(L, M)$ versus $X(L, M)$ and $Y(L, M)$, respectively, should give straight lines independently of the aspect ratio (L/M). Figure 6a and b show these plots and the excellent data collapsing obtained again confirms the validity of our conjecture. The values of p_c obtained at the intersections $X(L, M)=0$ and $Y(L, M)=0$ in Fig. 6a and b, respectively, are listed in Table 1.

IV.b. The largest cluster at criticality

As it has been pointed out in the previous section, the probability of a site belonging to the largest cluster $P_{L,M}(p)$ depends on two scaling variables, namely L/M and $\varepsilon\equiv(p-p_c)\,L^{1/\nu}$ (see Eq. (4)). Therefore, in order to test the scaling argument it is convenient to study the dependence on both variables separately. Figure 7 shows a log-log plot of $P_{L,M}(p)\,L^{\beta/\nu}$ versus L/M right at criticality, i.e. $\varepsilon=0$. One observes a reasonable data collapsing into a straight line behavior with slope $\delta\cong1$ as it has been conjectured in the previous section on the basis of finite-size scaling arguments. Nevertheless, a careful inspection of Fig. 7 suggests the existence of systematic deviations of the data corresponding to each constant values of L/M. This fact is stressed in Fig. 7 where two lines with slopes $\delta=1$ have been drawn for comparison; the full line passes through the points corresponding to $L=6$ while the dashed one is defined by points with $L=24$.

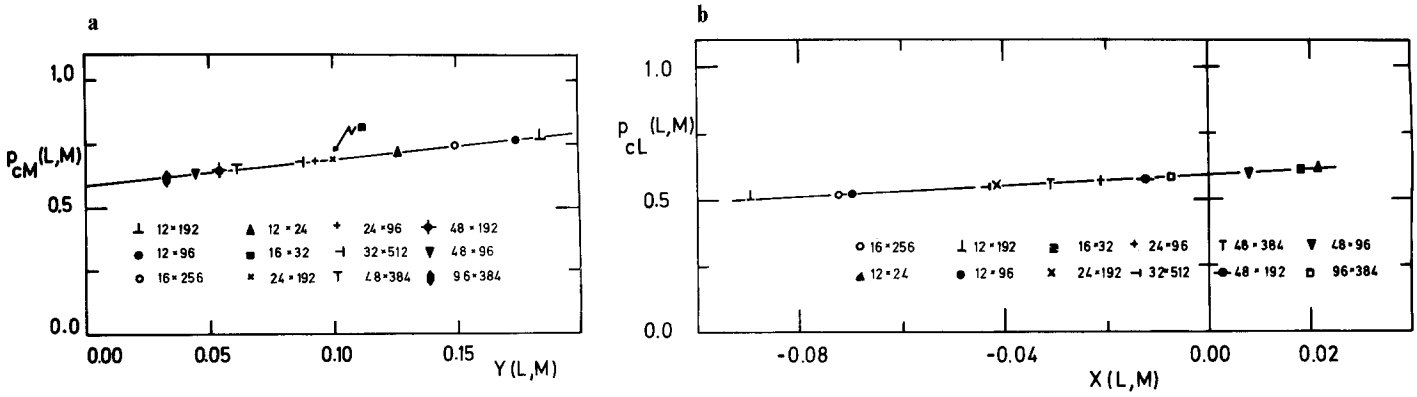

Fig. 6. a Plots of $p_{cM}(L, M)$ versus $Y(L, M)$ for lattices of different aspect ratio. **b** Same than **a** but for $p_{cL}(L, M)$ versus $X(L, M)$. The interceptions of the straight lines defined by the points for $X(L, M)=0$ and $Y(L, M)=0$ give the values of p_c listed in Table 1

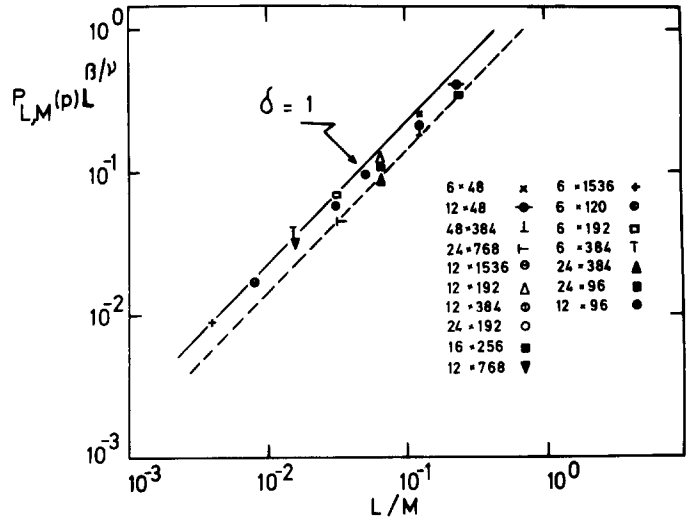

Fig. 7. Log-log plot of $P_{L,M}(p)\, L^{\beta/\nu}$ versus L/M for lattices of different aspect ratio. The straight lines with slope $\delta=1$ have been drawn for comparison. Note that the full (dashed) line is passes close to the points with $L=6$ ($L=24$), respectively

The observed deviations could be due to corrections to scaling which may play a role in small lattices. In fact the conjecture $\delta=1$ (see Eq. (8)) has been obtained assuming $M \propto L^{D_F}$ (Eq. (7a)), but taking into account finite-size scaling corrections, Eq. (7a) becomes

$$M(p=p_c) \cong A_1 L^{D_F} + A_2 L^{D_2} + \ldots \tag{15}$$

with $D_2 = D_F - 1$ in two dimensions [6]. So, assuming also corrections in (6) one can write

$$\phi_1(L/M) \cong (L/M)^{\delta} + \Phi_c \tag{16}$$

where the first term of the right hand side is the leading term with $\delta=1$ and the second one is the correction that has to be determined. Now, making similar replacements like those used in order to obtain (8) one gets, after some algebra

$$\Phi_c \propto M^{-1} \propto L^{-1}, \quad p=p_c, L/M=\text{cte}, \tag{17}$$

in qualitative agreement with the observed deviations.

On the other hand, the dependence of $P_{LM}(p)$ keeping the aspect ratio L/M constant have also been studied. Log-log plots of $P_{LM}(p)\, L^{\beta/\nu}$ vs ε (not shown here) exhibit data collapsing only for each set of lattices with the same aspect ratio, as expected from the discussion of Sect. III.

V. Conclusions

The standard percolation model in the square lattice is studied at criticality using a $L \times M$ geometry. Close to p_c, the constraint $L \ll M$ favors the growth of percolating clusters in the L-direction with respect to the M-direction. This finding is compared and discussed with a similar behavior observed in the ferromagnetic Ising model. Therefore, it is expected that in adsorption experiments on stepped surfaces one should observe the growth of adsorbed island crossing through the terraces, independently of the details of the adparticle-adparticle interaction energy. Scaling functions have an additional parameter, namely M, and consequently these functions also depend on the aspect ratio L/M. Using finite-size scaling arguments we conjectured the dependence on L/M of the scaling functions for both the percolation probability and the probability of a site belonging to the largest cluster ($P_{L,M}(p)$). These conjectures are tested by Monte Carlo simulations. Systematic deviations from scaling of the Monte Carlo data for $P_{L,M}(p)$ at constant aspect ratio are interpreted as due to a second order correction to the leading term. This kind of deviations are absent in the scaled plots of the percolation probability.

E.V.A would like to acknowledge stimulating discussions with Profs. K. Binder and D. Heermann

References

1. Stauffer, D.: Phys. Rep. **54**, 1 (1979)
2. Stauffer, D., Coniglio, A., Adam, A.: Avd. Polymer Sci. **44**, 103 (1982)
3. Stauffer, D.: In: Introduction to percolation theory. London: Taylor and Francis 1985

4. Herrmann, H.J.: Phys. Rep. **136**, 143 (1986)
5. Aharony, A.: Percolation. In: Directions in condensed matter physics. Grinstein, G., Mazenko, G. (eds.). Singapore: World Scientific 1986
6. Feder, J.: In: Fractals. New York: Plenum Press 1988
7. Heermann, D., Stauffer, D.: Z. Phys. B – Condensed Matter **40**, 133 (1980)
8. Martin, H.O., Albano, E.V.: Z. Phys. B – Condensed Matter **70**, 213 (1988)
9. Martin, H.O., Albano, E.V., Maltz, A.: J. Phys. A Math. Gen. **20**, 1531 (1987)
10. Albano, E.V., Binder, K., Heermann, D.W., Paul, W.: Z. Phys. B – Condensed Matter **77**, 445 (1989)
11. Albano, E.V., Binder, K., Heermann, D.W., Paul, W.: Surf. Sci. **223**, 151 (1989)
12. Albano, E.V., Binder, K., Heermann, D.W., Paul, W.: J. Chem. Phys. **91**, 3700 (1989)
13. Wandelt, K., Hulse, J., Küppers, J.: Surf. Sci. **104**, 212 (1981)
14. Davis, P.W., Quinlau, M.A., Somorjai, G.A.: Surf. Sci. **121**, 290 (1982)
15. Miranda, R., Daiser, S., Wandelt, K., Ertl, G.: Surf. Sci. **131**, 61 (1983)
16. Fink, H.W., Ehrlich, G.: Surf. Sci. **143**, 125 (1984)
17. Sokolowski, M., Pfnür, H.: Phys. Rev. Lett. **63**, 183 (1989)
18. Küppers, J., Seip, S.: Surf. Sci. **119**, 291 (1982)
19. Albano, E.V., Martin, H.O.: Phys. Rev. **B35**, 7820 (1987); **B38**, 7932 (1988)
20. Wagner, H.: Physical and chemical properties of stepped surfaces. In: Springer Tracts in Modern Physics. Vol. 85, Höhler, G. (ed.). Berlin, Heidelberg, New York: Springer 1979